De-risking the Polymorph Landscape: The Complex Polymorphism of Mexiletine Hydrochloride

Jessica L. Andrews[a], Sten O. Nilsson Lill[b], Stefanie Freitag-Pohl[a], David C. Apperley[a], Dmitry S. Yufit[a], Andrei S. Batsanov[a], Matthew T. Mulvee[a], Katharina Edkins[c], James F. McCabe[d], David J. Berry,[†e] Michael R. Probert[f] and Jonathan W. Steed[a].*

(a) Department of Chemistry, Durham University, Durham DH1 3LE, UK. (b) Early Product Development and Manufacturing, Pharmaceutical Sciences, R&D, AstraZeneca, Pepparedsleden 1, SE-431 83, Mölndal, Sweden. (c) School of Health Sciences, University of Manchester, Manchester. (d) AstraZeneca, Macclesfield. (e) School of Medicine, Pharmacy and Health, Durham University, Durham (f) Chemistry, School of Natural and Environmental Sciences, Newcastle University, UK. Email: jon.steed@durham.ac.uk.

ABSTRACT: This work presents an updated solid form discovery approach to the polymorphism of the anti-arrhythmic drug mexiletine hydrochloride, in which experimental and computational techniques are combined to provide a rigorous characterisation of the solid-form landscape of this compound. The resulting solid forms were characterised by powder and single crystal X-ray diffraction, IR spectroscopy, DSC, and ^{13}C solid-state NMR. This approach reveals five solid form types of mexiletine hydrochloride. Forms 1, 2 and 3 are mutually enantiotropically related anhydrous polymorphs, with Form 1 the room temperature

stable form, Form 2 the high temperature form and Form 3 is the thermodynamically stable polymorph between 148 °C and 167 °C. The final two forms termed Types A and B comprise two large families of isomorphous channel solvates, including a fourth non-solvated form isostructural to the type A solvates. We report eleven modifications of each solvate, in which a diverse range of solvents are included in the channels, without changing the fundamental structure of the drug framework. These experimental results go hand-in-hand with computational crystal structure prediction (using the AstraZeneca crystal structure prediction approach), which together suggest that it is unlikely further non-solvated forms, at least with $Z' = 1$, will be discovered under ambient conditions.

INTRODUCTION

The polymorphs of an active pharmaceutical ingredient (API) can have very different physical and chemical properties, which impact pharmaceutically important parameters such as bioavailability, dissolution rate and tabletability. Therefore, the polymorphism of an API must be tightly controlled to ensure that the properties of the medicine are reliable.[1-2] The uncontrolled emergence of an unknown or undesirable solid form at any stage in the life-cycle of a pharmaceutical can drastically reduce the efficacy of the drug and incur severe knock on effects for patients and the manufacturer, as famously occurred with ritonavir.[3] For these reasons, pharmaceutical companies face significant regulatory and financial pressure to fully characterise the solid-state landscape of new APIs, for example as part of a new drug application (NDA) filing.[4-5] The most common method used to assess the solid-form landscape of a new API is a crystallization screen, in which the drug is crystallised from a wide range of solvents, or using a variety of crystallisation techniques to access the full range of kinetic and thermodynamic solid forms.[6-7] These experiments can either be undertaken manually or more recently, using high-throughput robotic systems that are significantly more efficient.[8-9] There

has also been significant work in computational crystal structure prediction, which can be used to support experimental crystal form screens by identifying potential missed forms and predicting the conditions that may access new polymorphs.[10-13]

In this work we apply state-of-the art solid form discovery methods to the polymorphism of mexiletine hydrochloride, an anti-arrhythmic drug used to treat patients with an irregular heatbeat[14] (Figure 1). Mexiletine hydrochloride is freely soluble in water and is formulated as a racemate in commercial Namuscla and Mexitil using the most stable non-solvated polymorph at ambient temperature. However, the two enantiomers have different pharmacokinetic profiles[15] and there has been significant research into the stereoselective synthesis and crystallisation of the drug.[16-22] Studies have shown that the enantiomeric excess of mexiletine can be determined by ^{1}H NMR spectroscopy using a chiral solvating agent, and that this method is much simpler than traditional chromatographic techniques.[23-24] The chloride counterion has also enabled characterisation using solid-state ^{35}Cl NMR spectroscopy, which has emerged as a powerful method for distinguishing between the polymorphs of chloride-containing drugs.[25-26]

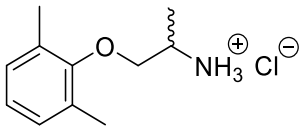

Figure 1. The structure of mexiletine hydrochloride.

Mexiletine HCl has been previously reported to have six solid forms, of which two crystal structures are published in the CSD.[25, 27-29] These forms have been characterised by IR spectroscopy, differential scanning calorimetry (DSC),[28-29] and in some cases, solid-state NMR spectroscopy.[25] DSC measurements show that mexiletine HCl is an enantiotropic system in which two unsolvated polymorphs, termed Modifikation I and II by Kuhnert-Brandstätter *et al.*[29] and Forms IV and VI by Kiss *et al.*,[28] are thermodynamically stable at different

temperatures.[28-29] The structure of the room temperature stable form (hereafter Form 1) was published in 1991 by Sivy *et al.*[27], but the high temperature stable form (hereafter Form 2) is yet to be crystallographically characterised. The crystal structure of Form 1 of mexiletine hydrochloride is racemic with two molecules per asymmetric unit, which share the same *gauche* conformation of the aliphatic chain. The crystal structure of a metastable form of mexiletine hydrochloride (hereafter Form 3) was published in 2016 by Namespetra *et al*.[25] This structure is also a racemate with only one molecule per asymmetric unit, which adopts a *gauche* conformation.

There has been considerable confusion in the literature and incomplete reports of the polymorphism of mexiletine hydrochloride and its polymorphism and solvatomorphism appears to be potentially very complex. In this work we aim to map the solid form landscape of this challenging drug and highlight not only how to reveal new forms of this compound but also when it is possible to be reasonably sure that all accessible forms have been discovered.

RESULTS AND DISCUSSION

Solid Form Screen

An extensive solvent-based solid form screen was undertaken on mexiletine hydrochloride in addition to further experiments involving sublimation and high pressure, *vide infra*. In contrast to the previous literature on mexiletine HCl the work reported herein reveals five types of solid forms of mexiletine hydrochloride. Three anhydrous polymorphs exhibiting mutually enantiotropic relationships that are stable at different temperatures, and two related families of metastable channel solvates. There also exists a non-solvated form isostructural to the type A solvateswhich represents a fourth unsolvated polymorph. In the solvate structures, the drug molecules form a porous framework that can accommodate an extensive range of solvents. These solvates can be divided into two broad families, based on the packing arrangement in

their mexiletine frameworks. Little change is observed in each of the host structures with a wide variety of guests as observed in previous channels[30-31] and in at least one case, the channel arrangement is retained in the absence of any solvent. Previous examples of this phenomenon have been reported.[32-33] Eleven solvates of each type have been prepared and given this highly prolific solvate formation it is likely that further solvates of similar structure exist. The large number of isomorphic solvates may account for the extra polymorph (total of six) identified by IR spectroscopy in a previous study,[28] as the incorporation of different solvents within the channels can significantly alter the IR spectrum of the material without inducing any significant structural change.

All previous studies have used different names to refer to the crystal forms of mexiletine. In this work, the non-solvated forms will be named according to their thermodynamic stability. The room temperature stable form is termed Form 1, the enantiotropically related high temperature stable form is termed Form 2 and the non-solvated metastable polymorph is termed Form 3. The previous nomenclature for these forms is summarised in Table S1. The two solvate families are termed Type A and B.

According to previous literature, Form 1 of mexiletine hydrochloride can be crystallised from ethanol and butanol.[27-28] In addition to these routes, our polymorph screen revealed that this form could also be accessed by slow and fast cooling (SC and FC), evaporation (EV) and anti-solvent precipitation (PPT) crystallisations, from a range of different solvents (

Table **1**). Single crystals of Form 2 were grown by sublimation at 150 °C, over a period of seven hours (Figure S1). This procedure is similar to the one reported by Hildebrand *et al.*, to access the high temperature form which they referred to as Mexi II.[26] Although in this case, the use of sublimation allows the formation of single crystals rather than a powder. Namespetra *et al.*[25] crystallised Form 3 by slow evaporation from acetone and in addition to this method, we have also crystallised this form by the evaporation of 1-propanol solution and fast cooling from

nitromethane, acetonitrile and ethyl acetate solutions. In these experiments, Form 3 crystallises concomitantly with Form 1 which suggests that these structures are close in energy or represent a combination of fast nucleation and fast growth[34] (Figure S2).

The Type A and B solvates were crystallised by slow and fast cooling, evaporation and precipitation from a wide range of solvent systems (

Table **1**). The fast cooling and precipitation methods often involved very rapid crystallisation, which prevented the growth of diffraction-quality single crystals. However, for solvates that were crystallised by precipitation, single crystals could often be grown using vapour diffusion to reduce the rate of anti-solvent addition. In some vapour diffusion experiments, the anti-solvent was changed from hexane to octane as it has a lower vapour pressure and further reduced the rate of anti-solvent addition. Some conditions lead to the concomitant crystallisation of more than one form. Precipitation from chloroform/hexane yields a mixture of a Type B solvate and Form 1. Similarly, a mixture of Type A and Type B solvates crystallises concomitantly by precipitation from DCM/hexane.

Table 1. Crystallisation conditions for all polymorphs of mexiletine.

Name	Crystallisation Technique
Form 1	As delivered **Slow cooling from:** chloroform ($CHCl_3$), ethyl acetate (EtAc), acetonitrile (AcN), nitromethane (NM), amyl alcohol (AmOH), 1-butanol (1BuOH), 2-butanol (2BuOH), 1-propanol (1PrOH), 2-propanol (2PrOH), ethanol (EtOH) **Fast cooling from:** $CHCl_3$, AmOH, 1BuOH, 2BuOH, 1PrOH, 2PrOH, EtOH **Precipitation from:** 1BuOH/hexane, EtOH/hexane, MeOH/hexane **Evaporation of:** $CHCl_3$, 1BuOH, 2BuOH, 2PrOH, EtOH, MeOH, AcN
Form 2	Heat any other form above its transition temperature or, sublimation at 150 °C
Form 3	A pure sample can be obtained by evaporation of acetone. A mixture with Form 1 can be obtained by: **Evaporation of:** 1PrOH **Fast cooling from:** NM, EtAc, AcN

Type A Solvates	**Slow cooling from:** Toluene (Tol), dichloromethane (DCM), MeOH **Fast cooling from:** Tol **Precipitation from:** 1PrOH/hexane, AmOH/hexane, dimethyl formamide (DMF)/diethyl ether, 2BuOH/hexane, 2PrOH/hexane **Evaporation of:** DCM
Type B Solvates	**Slow cooling from:** acetone (AcO), ethyl methylketone (EMK), THF, dioxane (Dio) **Fast cooling from:** AcO, Dio, THF, DCM, EMK **Precipitation from:** $CHCl_3$/hexane (mixture with Form 1)
Both solvated forms crystallise concomitantly by precipitation from DCM/hexane	

The five solid forms of mexiletine HCl were identified by PXRD, using the program PolySNAP[35-36] to group the patterns together by similarity. To ensure this analysis was accurate, only high-resolution PXRD patterns were used, and mixtures or low crystallinity samples (assessed by manual examination of the PXRD pattern) were discounted. The discounted samples include Type A solvates crystallised by precipitation from $CHCl_3$ or DCM/hexane and Type B solvates crystallised by fast cooling from DCM or THF and slow cooling from 1,4-dioxane. At a similarity coefficient of 0.65, the patterns were divided into five distinct clusters, except for the Type A methanol solvate. This similarity coefficient was chosen so that the known solid forms are separated into different clusters. At this level the PolySNAP clustering suggests that the methanol solvate is unrelated to any other form (

Figure **2**), although on the basis of structural similarity it is a member of the Type A solvates. At a similarity coefficient of 0.65, the PXRD patterns of Forms 1, 2 and 3 are all unique. However, at similarity coefficient of 0.6, Form 2 falls into the same cluster as the Type B solvates, which shows that these two forms are structurally related. Within both solvate clusters, there are various sub-groups with higher similarity coefficients. The highest similarity sub-groups often contain the same solvate crystallised by different methods whereas more differences are observed between solvates containing different solvents.

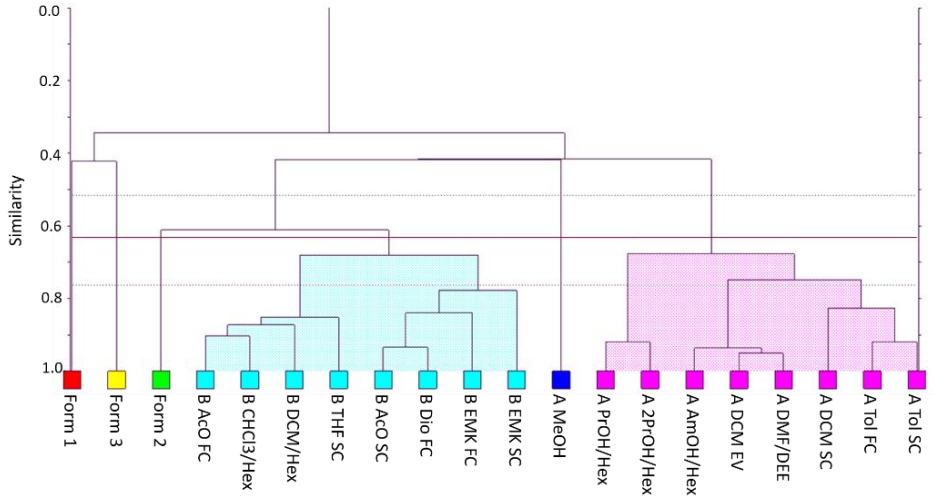

Figure 2. The PolySNAP packing similarity dendrogram. The red line at 0.65 shows the similarity coefficient that was used to cluster the patterns into the groups highlighted by different colours.

A similar clustering analysis was carried out on the single crystal structures of Forms 1, 2, 3 and seven of the Type A solvates characterised by single crystal X-ray diffraction (*vide infra*), using the CSD-Materials module in Mercury.[37] The packing similarity analysis generates a cluster of 20 molecules to represent each crystal structure.[38] Pairs of clusters are overlaid and the resulting root mean square deviation ($RMSD_{20}$) can be used to quantify differences between the two forms (Table S2). If all of the molecules in both clusters overlap, an $RMSD_{20}$ value of less than 0.6 Å shows that the two structures are the same,[13] and based on these results, Mercury separates the crystal structures into groups representing each polymorph.

The packing similarity analysis produced the same clusters as PolySNAP. Compared with all other crystal structures, Forms 1, 2 and 3 have unique packing arrangements and only one or two molecules overlap out of the group of 20. Similarly, all the structurally characterised Type A solvates have the same packing arrangement, except for the methanol solvate. The methanol solvate has the same packing arrangement as the Type A solvate crystallised from DMF/diethyl ether, with 20 out of 20 molecules overlapping and an $RMSD_{20}$ value of 0.576

Å. However, differences are observed between the methanol solvate and the four solvates crystallised by precipitation with an alkane anti-solvent. In these comparisons, 19 or 20 out of 20 molecules overlap, with $RMSD_{20}$ values slightly above the cut-off: between 0.65 and 0.79 Å. These results highlight slight structural differences in the drug framework of the methanol solvate arising from the ordered solvent molecules, which contribute to differences in the PXRD pattern of this form.

Structures of The Non-Solvated Forms of Mexiletine

Single crystals of Form 2 of mexiletine HCl were grown by sublimation at 150 °C. Selected crystallographic information for this structure is given in Table 2, along with the other non-solvated forms previously reported for reference. Full crystallographic information for Form 2 can be found in Table S7.

Table 2. Selected crystallographic information for the non-solvated forms of mexiletine.

	Form 1[27]	**Form 2**	**Form 3**[25]
Space Group	$P\bar{1}$	*Pccn*	*Pbcn*
a/Å	8.796(15)	17.874(14)	35.116(2)
b/Å	10.601(18)	18.678(15)	7.740(5)
c/Å	14.229(24)	7.346(7)	9.154(5)
α/°	78.74(13)	90	90
β/°	79.89(14)	90	90
γ/°	68.69(12)	90	90
V/Å^3	1204.3	2452.6(4)	2488.1(3)
Z	4	8	8
ρ_{calc} g/cm^3	1.19	1.17	1.15

As in all previously known structures of mexiletine, Form 2 is a racemic hydrochloride salt. The mexiletine cation in the structure is disordered and the model contains two different conformations of the mexiletine molecule (Figure S3). The *anti*-periplanar conformer, which has an O-C-C-N torsion angle of 174.5°, has an occupancy of 0.63. Whereas the *gauche* conformer, which has an O-C-C-N torsion angle of 47.8°, has an occupancy of 0.37. There are 56 entries in the CSD containing this R-O-CH_2-CHR-NH_3^+ fragment, in which the O-C-C-N torsion angles range from 44.1° to 75.4° (Figure S4). These angles all correspond to a *gauche* conformation, which suggests that the *anti*-periplanar conformer is less stable, see the section on conformational polymorphism below.

In Forms 2 and 3, there are three hydrogen bonds per chloride ion from the ammonium cations in adjacent molecules, forming a hydrogen-bonded polymer along the crystallographic *c*-axis. The molecules within this polymer are arranged in a square in both Forms 2 and 3, although the symmetry of this motif is different from on eanother. In Form 2, the molecules are related by two perpendicular *c*-glide planes, which intersect in the middle of the square (**Figure 3**).

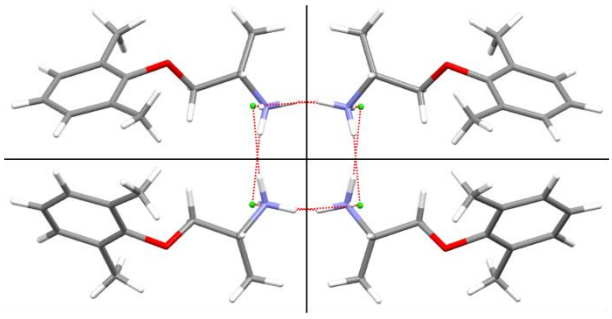

Figure 3. Form 2 of mexiletine, viewed down the *c*-axis. The *c*-glide planes are shown by black lines. For clarity, only the higher occupancy *anti*-periplanar conformer is displayed.

Although Forms 2 and 3 have similar packing arrangements, Form 1 is very different (Figure 4). When viewed down the hydrogen-bonded polymer chain axis (the *a*-axis for Form 1 and

the *c*-axis for Forms 2 and 3) the structures are all layered. In Form 1, the polymers align with each other in the *b*-direction but are offset in *c* due to the shape of the triclinic unit cell. Forms 2 and 3 are both orthorhombic and the molecules align in both the *a*- and *b*-directions. In both these structures, the layers are shifted such that the chains line up in every other layer.

(a) Form 1

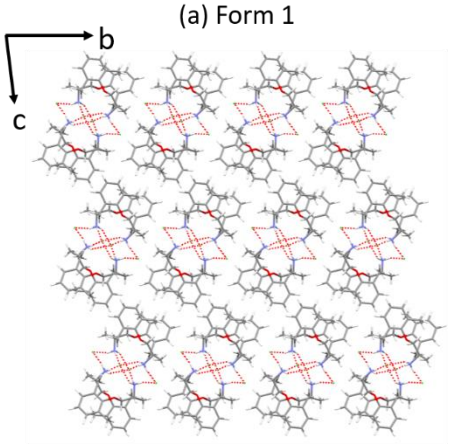

(b) Form 2

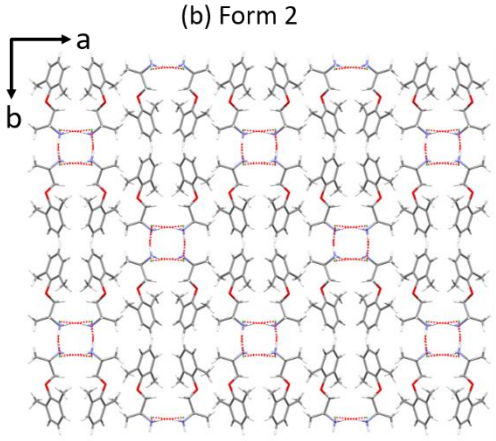

(c) Form 3

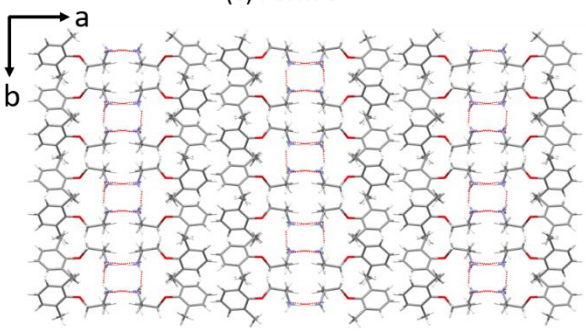

Figure 4. The packing arrangements of Forms 1, 2 and 3 of mexiletine, viewed down the hydrogen-bonded chains, which corresponds to the crystallographic (a) *a*-axis and (b,c) *c*-axis. For clarity, only the higher occupancy *anti*-periplanar conformer in Form 2 is displayed.

IR spectroscopy was also used to characterise the non-solvated forms of mexiletine. The major differences between their spectra occur in the ammonium NH and CH stretching region between 3300 and 2300 cm^{-1}, which is unique for each of Forms 1, 2 and 3 (Figure 5).

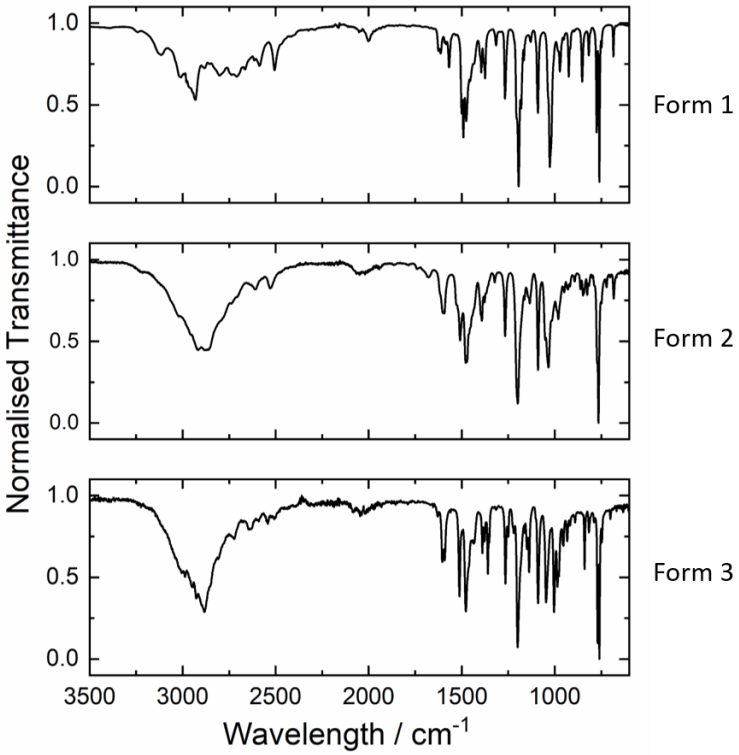

Figure 5. IR spectra of Forms 1, 2 and 3 of mexiletine. Form 1 was used as delivered, Form 2 was crystallised by sublimation at 150 °C and Form 3 was crystallised by evaporation of acetone.

Thermodynamic Relationships Between the Non-Solvated Forms of Mexiletine Hydrochloride

The thermodynamic relationships between the three non-solvated forms of mexiletine hydrochloride were investigated by DSC (Figure 6, Table 3). These findings mirror previous reports[28-29] in which all polymorphs transform into Form 2 upon heating, which then melts at 202 °C. Hence, Form 2 is the only form that does not display a polymorphic transition or desolvation endotherm upon heating. The polymorphic transition in Form 1 has an observed onset temperature of 148 °C and an enthalpy of 8.4 kJ mol^{-1}, whereas Form 3 transforms into Form 2 at an observed onset temperature of 167 °C and with an enthalpy of 4.5 kJ mol^{-1}. Although Form 3 is metastable at room temperature, it has a higher polymorphic transition temperature than Form 1 while the enthalpy of transition is lower. Therefore, Form 3 is likely to be the most stable form between the polymorphic transition temperatures of Form 1 and Form 3, *i.e.* between 148 and 167 °C. This means that all three transitions are enantiotropic even though none of the reverse transitions can be observed. The structure of Form 3 is more similar to Form 2 and therefore, less molecular reorganization is required to achieve the Form 3 to Form 2 transformation, which is likely to be responsible for its lower transition enthalpy.

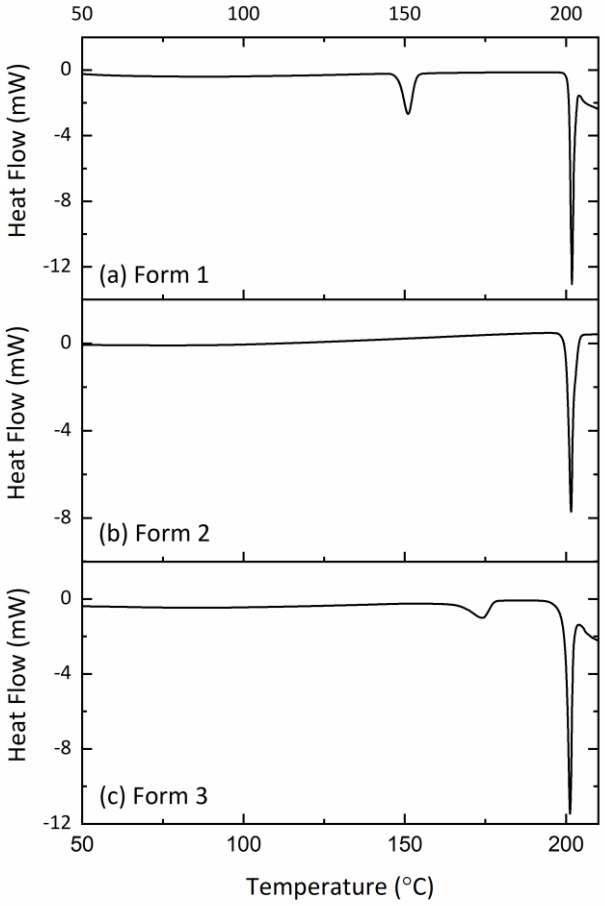

Figure 6. DSC thermograms of (a) Form 1, (b) Form 2 and (c) Form 3 of mexiletine. Endothermic events are portrayed down.

Table 3. The temperature and enthalpy of each transition in the DSC thermograms of Forms 1, 2 and 3 of mexiletine. Differences in measured melt enthalpy represent experimental variability since each sample transforms to Form 2 before melting.

	Polymorphic transition			**Melting point**		
	Onset / °C	**Peak / °C**	**ΔH / kJ mol^{-1}**	**Onset / °C**	**Peak / °C**	**ΔH / kJ mol^{-1}**
Form 1	148	151	8.4	201	202	16.7
Form 2	-	-	-	200	202	18.6
Form 3	167	174	4.5	200	202	16.2

Structures of the Solvated Forms of Mexiletine

Each family of channel solvates is characterised by a specific series of peaks in their PXRD patterns. These peaks are mostly observed at low angles and are consistent between all solvates of the same family. At higher angles there are some extra peaks or shifts between the patterns, which correspond to changes in the channel dimensions or the presence of different crystalline solvents within the pores. However, the similarities between all members of the same family are sufficient to qualify them as the same structure type.[30-31]

In the PXRD patterns of the Type A solvates, the characteristic peaks occur in the regions 6-7, 8-10, 13-14 and 15-16° 2θ and only shift slightly in position between each solvate (Figure 7). These patterns match closely at higher angles, except for the solvates crystallised from 1- and 2-propanol, which contain some extra peaks between 17 and 27° 2θ. It was not possible to obtain an experimental PXRD pattern of the Type A methanol solvate because the crystallisation requires such a high degree of supersaturation that when the crystals are removed from the mother liquor, Form 1 immediately precipitates from solution, forming an inseparable mixture. As such, the PXRD pattern calculated from the single-crystal structure was used for comparison and it also matches closely with the rest of the group.

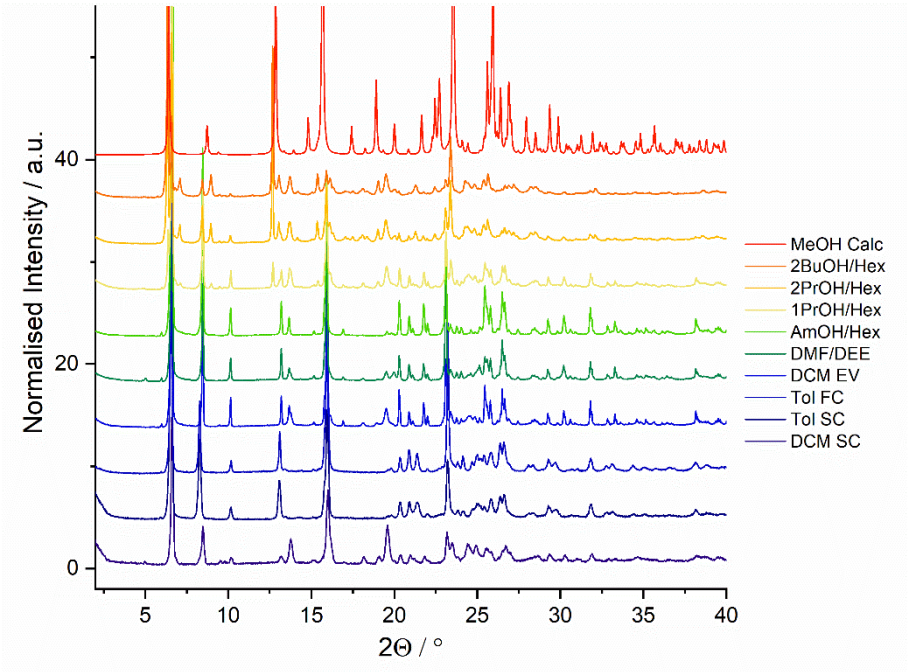

Figure 7. PXRD patterns of all Type A solvates. The crystallisation conditions are as follows, from the bottom up: slow cooling from DCM, slow cooling from toluene, fast cooling from toluene, evaporation from DCM, precipitation with diethyl ether from DMF, precipitation with hexane from amyl alcohol, precipitation with hexane from 1-propanol, precipitation with hexane from 2-propanol, precipitation with hexane from 2-butanol and slow cooling from methanol. The methanol pattern was calculated from the crystal structure.

In the PXRD patterns of the Type B solvates, the characteristic peaks occur in the regions 6-7, 9-10, 13-14, 15-17, 19-20 and 23-25° 2θ (Figure 8). However, there is some subtle variation in the shape and position of the peaks at approximately 6° and between 15-18° 2θ. The PXRD patterns of the Type B solvates are strongly affected by preferred orientation, causing the intensity of several peaks to vary significantly. This effect is most noticeable for the peaks at approximately 5, 6, 13 and 16° 2θ. As in the Type A solvates, differences are observed between the Type B patterns at higher angles, particularly between 15 and 30° 2θ. Some of the Type B solvates were crystallised by fast cooling, which leads to reduced crystallinity, broadened peaks, and a lower signal to noise ratio in their PXRD patterns. This effect is most noticeable

for the samples crystallised by fast cooling from DCM and EMK. However, the similarities in their key peaks between 13 and 27° 2θ are sufficient to qualify them as Type B solvates.

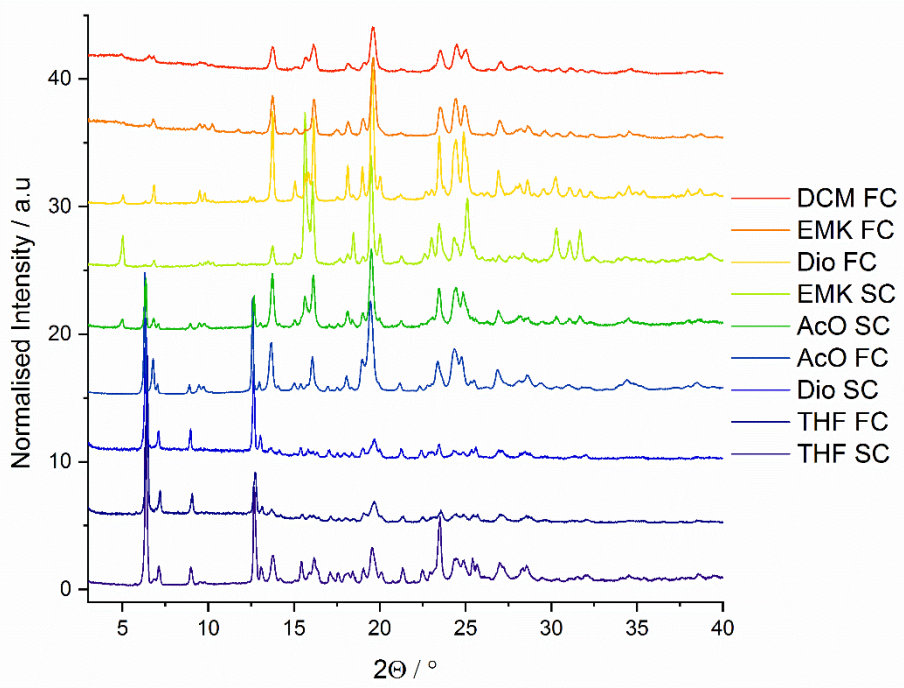

Figure 8. PXRD patterns of all Type B solvates. The crystallisation conditions are as follows, from the bottom up: slow cooling from THF, fast cooling from THF, slow cooling from 1,4-dioxane, fast cooling from acetone, slow cooling from acetone, slow cooling from EMK, fast cooling from 1,4-dioxane, fast cooling from EMK, and fast cooling from DCM.

Single-crystal structures of seven Type A solvates were determined. Although the dimensions of the channels and therefore the unit cells (

Table 4), vary slightly with the incorporation of different guests, their overall packing arrangement varies very little. This behavior has been also observed for other pharmaceutical solvates.[30-31] Full crystallographic information for all of these forms can be found in Tables S8-12.

Table 4. Selected crystallographic information for the Type A solvates.

Crystallisation Conditions	DCM SC slow cooling	MeOH SC slow cooling	1PrOH/octane vapour diffusion	2BuOH/octane vapour diffusion	2PrOH/hexane vapour diffusion	DCM/hexane vapour diffusion	DMF/diethyl ether vapour diffusion
Space group	*Pbcn*	*Pbcn*	*Pbcn*	*Pbcn*	*Pbcn*	*Pbcn*	*Pbcn*
a/Å	20.857(2)	20.243(7)	21.936(13)	21.924(14)	21.875(17)	21.456(3)	21.125(2)
b/Å	17.378(18)	18.768(6)	17.106(10)	17.110(11)	17.211(13)	17.333(2)	17.358(16)
c/Å	7.565(8)	7.550(2)	7.521(5)	7.520(5)	7.511(6)	7.5478(11)	7.563(7)
α/°	90	90	90	90	90	90	90
β/°	90	90	90	90	90	90	90
γ/°	90	90	90	90	90	90	90
V/Å^3	2741.9(5)	2868.4(15)	2822.3(3)	2820.8(3)	2827.9(4)	2807.0(7)	2773.1(4)
Z	8	8	8	8	8	8	8
ρ_{calc} g/cm^3	1.045	1.147	1.015	1.016	1.013	1.021	1.033

The solvent-free form of the Type A solvates was crystallised by slow cooling a supersaturated solution in DCM. This form is isostructural with the rest of Type A solvates but in this case, the pores are empty, making this structure a fourth non-solvated polymorph of mexiletine.[39] As in Forms 2 and 3, the solvent-free structure is a racemate and the asymmetric unit contains one mexiletine molecule. This molecule adopts a *gauche* conformation, with an O-C-C-N torsion angle of 60.8º, which is in line with similar structures with this type of functionality in the CSD. Each ammonium cation hydrogen bonds to three chloride counterions, forming a hydrogen-bonded polymer along the crystallographic *c*-axis, in which the molecules are arranged in a square formation with the same symmetry as Form 3. Down the *a*- and *b*-axes, the packing arrangement in the solvent-free Type A structure is also very similar to Form 3, although the molecules are oriented differently (Figure S5).

The defining features of the solvent-free Type A structure are the large, continuous voids running along the crystallographic *c*-axis (Figure 9). Calculated using the inward-facing surface of a spherical 1.4 Å^3 probe,[40] the voids occupy 255 Å^3 per unit cell or, 9.3 % of the crystal volume. This volume reduces to 39.88 Å^3 or 1.5 % when only the solvent-accessible voids, mapped using the centre of the spherical probe, are considered. This estimate of the solvent-accessible volume within this crystal structure is likely to be conservative because Mercury uses hard spheres to model both the host framework and the included solvent. In reality, both the solvent molecules and the host framework have a more nuanced shape and some degree of flexibility, which allow a larger volume of solvent to be included within the channels.[41]

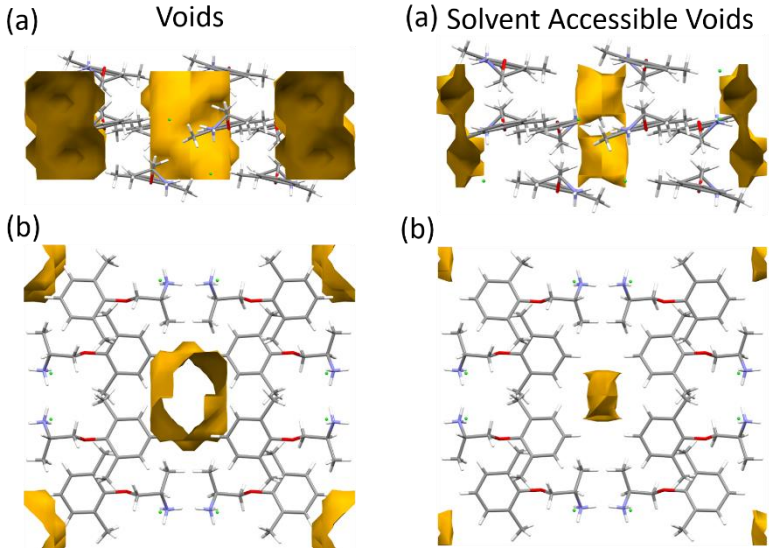

Figure 9. The void structure in the solvent-free Type A form of mexiletine, viewed down the (a) *a*-axis and (b) *c*-axis. The voids are highlighted in yellow and were calculated in Mercury using a 1.4 Å^3 spherical probe.[40]

Both types of void are continuous, but the solvent-accessible voids are small and narrow, which means only small or linear solvents can be included as guests. The surface of the channels is lined by mexiletine's aromatic rings, creating a hydrophobic environment that

favours the inclusion of hydrophobic solvents. It is most likely the steric bulk of these aromatic groups that promotes a low-density packing arrangement in this form, stabilised by the strong charge-assisted hydrogen bonds from the ammonium groups. No solvent masking procedure was employed during the refinement of the solvent-free structure, and SQUEEZE[42] indicates a residual electron density in the channels of only 6 electrons per unit cell. Hence, the voids really are devoid of crystalline solvent. The experimental PXRD pattern of the solvent-free form matches exactly with the calculated pattern from the crystal structure and is repeatable over several experiments (Figure S6).

The Type A methanol solvate is the only crystal structure of this family that contains well resolved, ordered solvent within the channel, and the only disorder in this structure can be modelled by two positions of the alcohol OH proton. The methanol molecules do not interact with the host framework and instead hydrogen bond with each other, forming separate chains along the crystallographic *c*-axis (Figure 10). An electrostatic potential (ESP)-plot of the solvent channel was created on a system created of sixteen molecules from the solvent-free Type A structure. The plot shows the nonpolar character of the void as illustrated by the green colour of the area nearest the void. Due to this hydrophobic channel surface, the methanol molecules pack with their alcohol groups facing inwards towards each other and their methyl groups facing outwards towards the channel. Full crystallographic information for this structure can be found in Table S9.

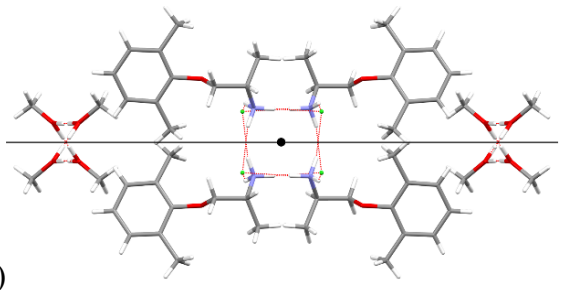

(a)

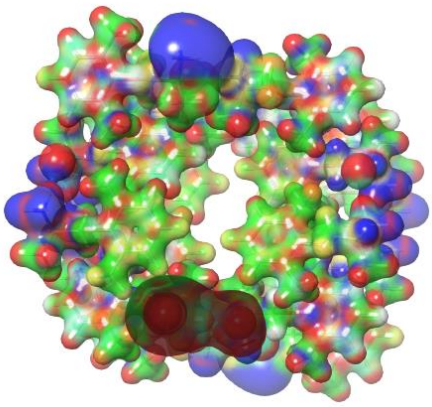

(b)

Figure 10. (a) The Type A methanol solvate of mexiletine, viewed down the *c*-axis. The centre of inversion is shown as a black circle and the *c*-glide plane is shown as a black line. (b) Electrostatic potential (ESP) plot for solvent-free Type A structure computed at B3LYP/6-31g(d,p) level of theory with the colour scale of -398.8 kJ/mol (red) to +459.5 kJ/mol (blue).

The host frameworks in the Type A methanol solvate and the solvent-free form are isostructural. Both structures consist of offset layers, which alternate every half unit cell in both the *a*- and *b*-directions, so that the channels line up every other layer (Figure 11). However, there are slight differences in the unit cell dimensions of these two forms. In the methanol solvate, the *a*-axis is shorter and the *b*-axis is longer, showing that the channel dimensions have changed to accommodate the solvent molecules (Table 4

Table 4).

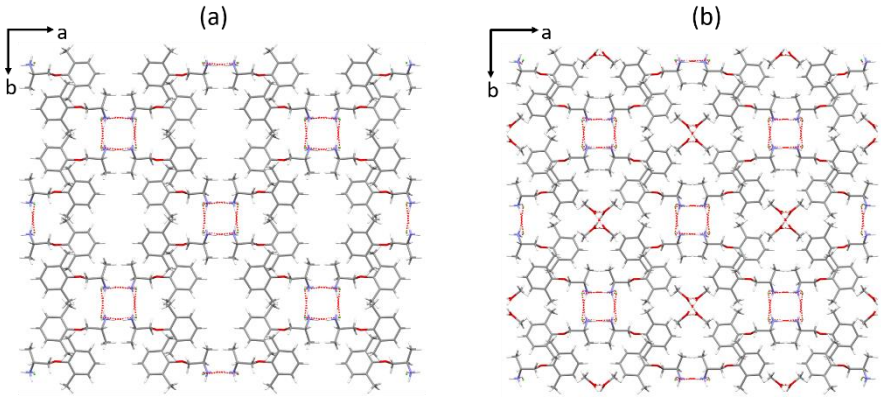

Figure 11. The packing arrangement of (a) the solvent-free Type A form and (b) the Type A methanol solvate, viewed down the *c*-axis.

The crystal structures of five isostructural Type A solvates were determined using crystals grown by vapour diffusion of hexane, octane, or diethyl ether into a supersaturated solution of mexiletine HCl in 1-propanol, 2-propanol, 2-butanol, or DMF. Full crystallographic information for these materials can be found in Table S10. As with the methanol solvate, slight variations in the cell dimensions of these compounds occur perpendicular to the channels, signifying a change in the channel dimensions to accommodate various solvents (

Table 4). In all these structures, the solvent molecules are highly disordered and were taken into account using a solvent masking procedure. The Mercury packing similarity analysis (Table S2) shows that the structure of the host framework in the solvates grown by vapour diffusion is slightly different to the methanol solvate. This difference is likely to arise as a result of the ordered solvent within the pores of the methanol solvate interacting with the channel walls, in contrast to the disordered guests present in the other forms.

One single-crystal structure of a Type B solvate was determined using a crystal grown by slow cooling from a supersaturated solution in ethyl methyl ketone, EMK. It is extremely disordered (Figure S7) and although several attempts were made to grow a better-quality crystal, these solvates crystallised exclusively as tiny needles that were very weakly diffracting. As a result, the precision of this structure is poor, but the approximate model does give insight into the gross structural features. The unit cell dimensions of this structure are given in**Table 5**.

Parameter	**EMK B slow cooling**
a/Å	27.91(2)
b/Å	27.91(2)
c/Å	7.515(8)
α/°	90
β/°	90
γ/°	90
Space group	$P4_2bc$

Table 5. Unit cell dimensions of the Type B EMK solvate of mexiletine hydrochloride derived from slow cooling.

The Type B EMK solvate is a 2:1 hemisolvate, with two mexiletine molecules per asymmetric unit. As in all other metastable polymorphs, the ammonium groups hydrogen bond to chloride anions, forming a hydrogen-bonded polymer along the crystallographic *c*-axis (Figure 12). However, in contrast to the other metastable forms, there are two different hydrogen bonding motifs in this structure. One consists of four molecules, related by a 4-fold axis, and connected by three hydrogen bonds per chloride anion. The other contains two pairs of molecules, related by two perpendicular *c*-glide planes, and connected by two hydrogen bonds per chloride anion. The latter motif has the same symmetry as the hydrogen-bonded polymers in Form 2, and although Form 2 has one more hydrogen bond per chloride ion, the arrangement of molecules within the two motifs is the same. The structural similarity between Form 2 and the Type B solvates was also observed in their PXRD patterns, highlighted by the PolySNAP similarity dendrogram (Figure 2).

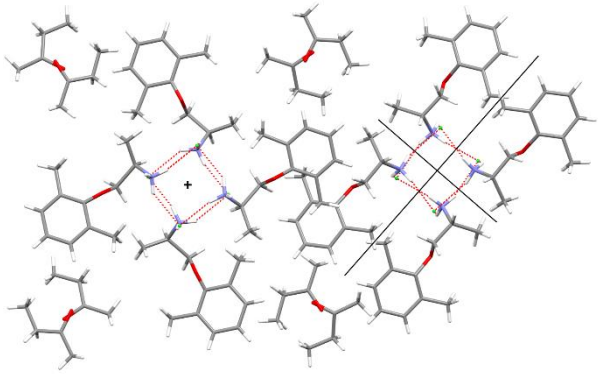

Figure 12. The Type B EMK solvate of mexiletine, viewed down the *c*-axis. For clarity, only one disordered component has been displayed. The *c*-glide planes are labelled as black lines and the 4-fold axis is labelled as a black cross.

As in the Type A solvates, the solvent molecules in the Type B EMK solvate are accommodated in channels within the host framework and do not interact significantly with the mexiletine cations. The surface of these channels is lined with aromatic rings, making them

hydrophobic and encouraging the solvent molecules to pack with their hydrophobic functionality facing the channel walls (Figure 13). This structure is layered, with every other layer containing solvent molecules. The layers alternate every quarter unit cell along both the *a*- and *b*-axes, so that the same structural features line up every fifth layer.

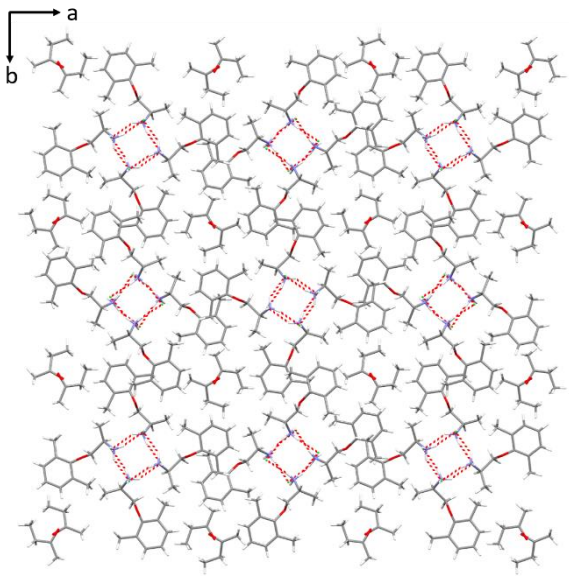

Figure 13: Packing arrangement of the Type B EMK solvate of mexiletine, viewed down the *c*-axis. For clarity, only one disordered component has been displayed.

Carbon-13 solid-state (SS) NMR spectroscopy was used to further characterise the channel solvates. Two excitation methods were used for each sample: cross-polarisation and direct-excitation. Cross-polarisation was used to assess the rigid, crystalline, parts of the structure, whilst short recycle, direct-excitation measurements were used to probe the more mobile, "liquid-like" components. As the solvates are metastable, the NMR samples were also characterised by IR spectroscopy and PXRD both before and after measurement of the NMR spectra, to ensure they had not transformed during the experiment. The expected mexiletine signals were observed in every cross-polarisation spectrum and for all samples apart from solvent-free forms, solvent signals were also visible in one or both spectra. These solvent resonances were used to determine the contents of every channel solvate, as shown in Tables

S3 and S4. A mexiletine signal is observed at approximately 14 ppm in all the direct-excitation spectra, corresponding to the aliphatic methyl group, which has a shorter carbon relaxation time than the other carbon atoms due to its high rotational freedom.

For most of the Type A solvates, solvent resonances were visible in both types of SS NMR spectra. However, they were much stronger by direct-excitation, which suggests that the solvent is highly mobile but not entirely liquid-like. All precipitation experiments that yielded a Type A solvate involved a polar, hydrogen-bonding solvent and a non-polar, aprotic anti-solvent. In every case, NMR data shows that the anti-solvent is contained within the channels, which is likely caused by the hydrophobic nature of the channel surface. In contrast, no solvent signals were observed in either SS NMR spectrum of the samples crystallised by slow cooling and evaporation of DCM, which highlights that both of these methods result in solvent-free Type A structures and confirms that the pores in this form are truly empty. The Type A solvates crystallised by fast and slow cooling from toluene are a particularly interesting case. The PXRD patterns of both samples match the pattern of the solvent-free form exactly, which suggests that the pores may be empty. However, toluene peaks are observed weakly in the cross-polarisation spectra and strongly in the direct-excitation spectra of these forms, which shows that the channels actually contain highly mobile toluene molecules that are too disordered to diffract X-rays (Figure 14).

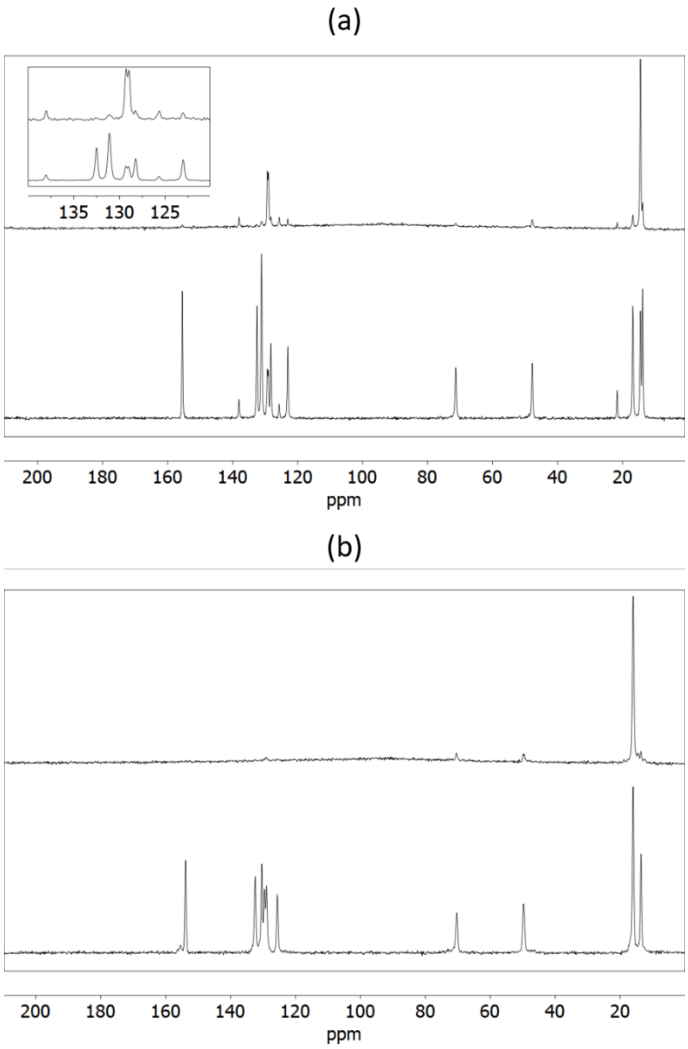

Figure 14. Solid-state NMR spectra of the Type A solvates of mexiletine, crystallised by slow cooling from (a) toluene and (b) DCM. In both cases, the top spectra were recorded using direct-excitation and the bottom spectra using cross polarization.

Solvent signals were also observed in the cross-polarisation and direct-excitation spectra of the Type B solvates. The signals were stronger in the cross-polarisation spectra, suggesting that the solvent in these structures has restricted mobility. This trend is reflected in the PXRD patterns of this form, which are much more varied than Type A, suggesting a larger variation in the crystalline components of the Type B solvates. A solvent-free Type B form was also identified by SS NMR, crystallised by fast cooling from DCM. No solvent signals were

observed in either NMR spectrum of this sample, showing that the pores are empty. Since the solvent-free Type A form was also produced by crystallisation from DCM, it is likely that while this solvent facilitates the crystallisation of channel solvates, it is too volatile and interacts with the hydrophobic channels too weakly to be retained.

Solid-state ^{13}C NMR spectroscopy could also be used to distinguish between the Type A and B solvates, and to distinguish them both from Form 1. This technique has previously been applied to distinguish between Forms 1, 2 and 3.[25] All spectra differ in the four fingerprint regions identified by Namespetra *et al.* between 154-156, 70-72, 47-49, and 10-20 ppm (Figure 15).[25] The spectra of the Type A solvates, which have one molecule per asymmetric unit, are always much simpler than those of Type B and Form 1, which have two molecules per asymmetric unit. For certain nuclei, signals from these two symmetry-independent molecules can be resolved by NMR spectroscopy, as seen at approximately 48 and 72 ppm. At 48 ppm, the two signals overlap and so the peak appears broad, with a small shoulder. There are also significant differences in the aromatic region between 120-135 ppm that are more characteristic of the solvates (Figure 15). Once again, the aromatic region is much simpler for the Type A solvates, including only the expected four signals, whereas the spectra of the Type B solvates and Form 1 contain more peaks, due to their higher values of Z'. All three forms can be distinguished by differences in the chemical shift, which was used to confirm the polymorphism of the poorly crystalline samples that produced low-resolution PXRD patterns as a result of the fast cooling crystallization of the Type B solvates (from acetone, DCM and EMK).

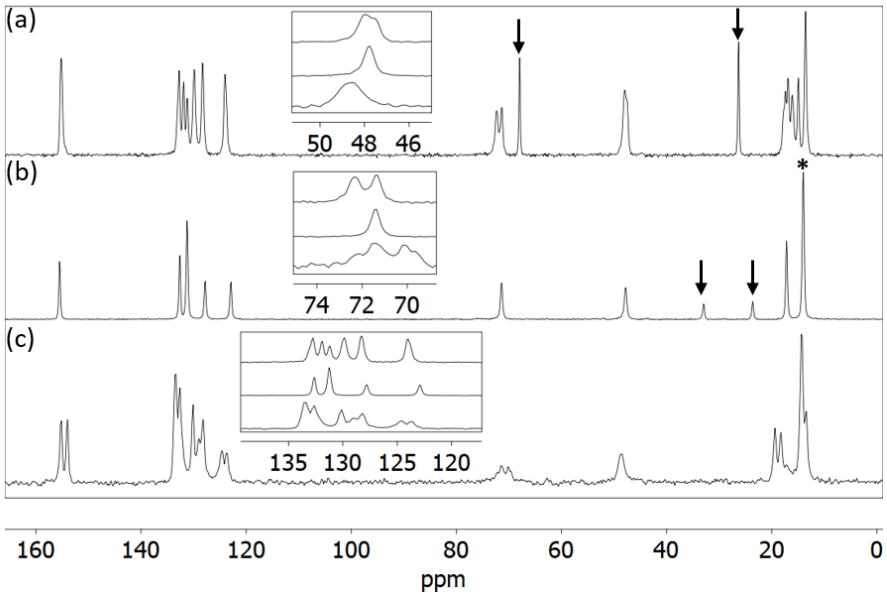

Figure 15. Cross-polarisation SS NMR spectra of (a) the Type B solvate crystallised by slow cooling from THF, (b) the Type A solvate crystallised by precipitation from amyl alcohol / hexane, and (c) Form 1 used as supplied. Solvent peaks are highlighted with arrows, corresponding to (b) hexane and (a) and THF. The hexane signal at 14 ppm in spectrum (b), highlighted with an asterisk, overlaps with a mexiletine signal, hence the higher intensity of this peak.

The structure of the mexiletine hydrochloride solvates was also characterised by IR spectroscopy. As with the non-solvated polymorphs, the IR spectra of the Type A and B solvates are very similar, and it was not possible to distinguish the two families by this method. Similarly, there is little variation between different solvates of the same family, showing that any slight changes in crystal packing cannot be resolved by IR spectroscopy. Representative IR spectra of the Type A and B solvates are shown in Figure S8 and these data were predominantly used as a convenient method to confirm the polymorphism of a sample before characterising it in more detail using another technique.. In the EMK and acetone solvates, the carbonyl stretch of the solvents are observed at 1715 and 1710 cm^{-1} respectively, and in the

dioxane solvates, the CH_2 twisting vibration of the solvent is observed at 1289 cm^{-1} (Figure S9).[43]

Thermodynamic Relationships Between the Solvated Forms of Mexiletine

Both solvate families are metastable with respect to Form 1. If removed from the mother liquor and stored under ambient conditions, the solvates transform into Form 1 over a time ranging from one hour to one day, depending on how the sample was crystallised and which solvent is included in the pores. If either of the channel solvates are subject to desolvation at increased temperatures, they transform into the high temperature stable Form 2, which was confirmed using PXRD (Figure S10).

DSC measurements showed that the desolvation transition to Form 2 occurs at a different temperature for each solvate. Representative DSC thermograms of each solvate family are shown in Figure 16. In some cases, the polymorphic transition is well defined, whereas in others it is very broad and often the data are not reproducible. Despite this variation, the melting endotherm in all samples occurs at approximately 202 °C, which corresponds to that of Form 2, and confirms that the transition has taken place. The broad peaks and inconsistent desolvation behaviour signify that the solvent is loosely bound within the channels. As a result, the solvent content will vary between different samples and may change over time if the sample was stored prior to measurement, leading to differences in the desolvation endotherm. This effect may be compounded in the Type B solvates due to their structural similarity with Form 2, which means that very little molecular rearrangement is required to change between the two forms, and the transition has a low enthalpy. This factor, coupled with the possibly variable solvent occupancy contributes to the fact that the desolvation endotherms are much broader in the Type B solvates than Type A.

Similar inconsistencies were also observed when the solvates were characterised using TGA. The measurement was repeated multiple times for each solvate, and rarely led to consistent results, suggesting that in many cases the solvent is non-stoichiometric and loosely bound within the channels.

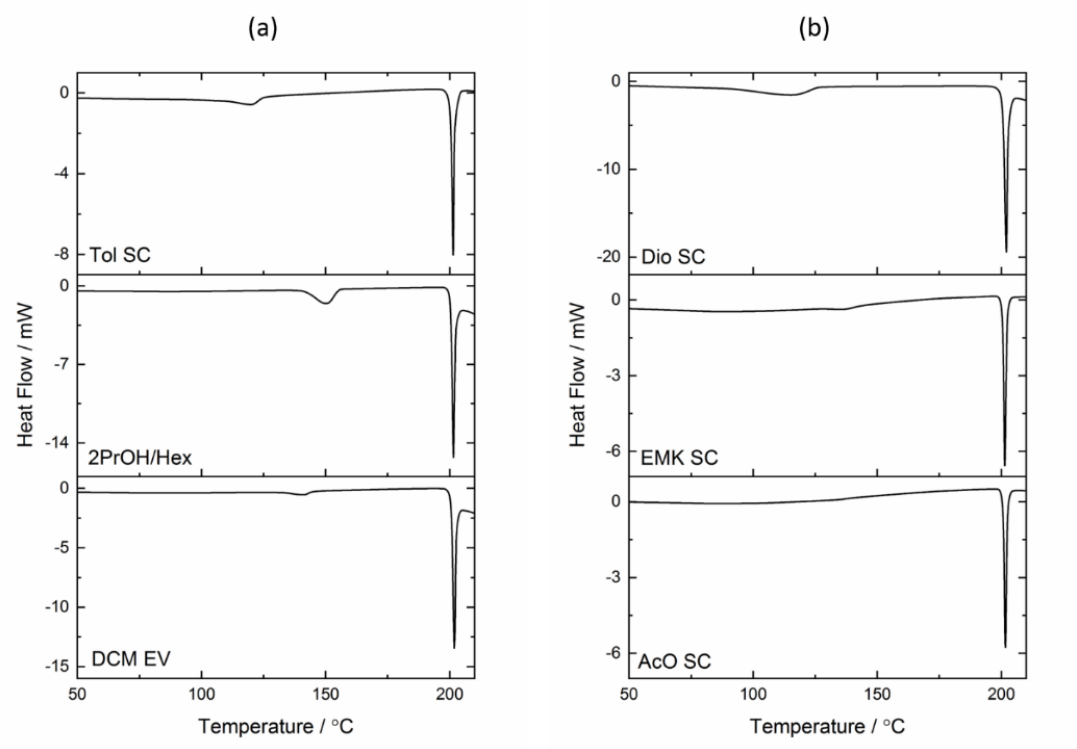

Figure 16. DSC thermograms of (a) three Type A solvates, crystallised by slow cooling from toluene, precipitation from 2-propanol/hexane and evaporation from DCM (b) three Type B solvates, crystallised by slow cooling from dioxane, EMK and acetone.

Table 6. The enthalpy and onset temperature of each transition in the DSC thermograms shown in **Figure 16**.

	Desolvation		**Melting point**	
	Onset / °C	**Peak / °C**	**Onset / °C**	**Peak / °C**
A Tol SC	104	120	201	201
A 2PrOH/Hex	142	150	201	202
A DCM EV	133	141	196	202
B Dio SC	85	115	201	201
B EMK SC	-	-	201	201
B AcO SC	-	-	201	202

Characterisation of Mixtures

Concomitant crystallisation of multiple forms was observed in precipitation experiments from $CHCl_3$/hexane and DCM/hexane. PXRD data shows that the sample crystallised from $CHCl_3$/hexane is a mixture of Form 1 and a Type B solvate (Figure S11a). The Type B solvate rapidly transforms into Form 1 and as a result, it was not possible to characterise this form by SS NMR. The mixture crystallised from DCM/hexane contained large and small crystals. Single-crystal X-ray diffraction revealed the larger crystals to be a Type A solvate containing highly disordered electron density within the pores (

Table 4). There were no residual peaks large enough to correspond to a chlorine atom of DCM and so the solvent was assumed to be hexane, which mirrors the behaviour of other Type A solvates crystallised by precipitation. The smaller crystals did not allow the determination of a full structure, but their unit cell (Table 7) and PXRD pattern (Figure S11b) showed them to be a Type B solvate.

Table 7. Unit cell dimensions of the Type B solvate crystallised by vapour diffusion of hexane into DCM, compared to the Type B EMK solvate crystallised by slow cooling.

Crystallisation Conditions	**EMK SC slow cooling**	**DCM/hexane vapour diffusion**
a/Å	27.91(2)	27.74(2)
b/Å	27.91(2)	27.72(2)
c/Å	7.515(8)	7.473(12)
α/°	90	90
β/°	90	90
γ/°	90	90

The cross-polarisation SS NMR spectrum of this mixture contained signals from both DCM and hexane, but only hexane was observed by direct-excitation (Figure S12). As the hexane molecules were attributed to the Type A solvate, this data suggests that the Type B solvate contains crystalline DCM within the pores. Given that solvent-free forms of both the Type A and B solvates were crystallised from DCM, it is surprising that crystalline DCM was found within this Type B solvate. Perhaps the addition of hexane to the solvent mixture provides a means to stabilise this unusual structure.

Conformational Polymorphism

The molecular conformations in all forms of mexiletine, except for the highly disordered Type B EMK solvate, are shown in Figure 17.

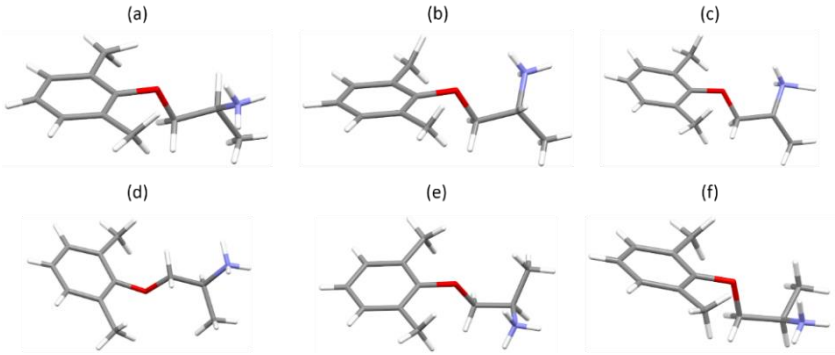

Figure 17. The molecular conformation in (a) molecule 1 of Form 1, (b) molecule 2 of Form 1, (c) the *gauche* conformer of Form 2, (d) the *anti*-periplanar conformer of Form 2, (e) Form 3 and (f) the solvent-free Type A form.

The differences between these conformations were quantified using Mercury.[37] Two equivalent atoms in a pair of molecules from different crystal structures were overlaid, producing a root mean square deviation (RMSD) for their atomic positions. A review of nearly 3000 crystal structures from the CSD concluded that for two conformations to be considered unique, they require an RMSD greater than 0.375 Å.[44] The results of these comparisons can be

found in Table S5. These results show that the non-solvated polymorphs of mexiletine, Forms 1, 2 and 3, are conformational polymorphs, producing RMSD values above the threshold.[44] The lower occupancy, *gauche* conformer of Form 2 is an exception, and shares its conformation with Form 1. However, as the higher occupancy, *anti*-periplanar conformer is significantly different to all the other forms, Form 2 can also be considered a conformational polymorph of the other non-solvated forms. The major difference between Forms 1, 2 and 3 is the position of the terminal ammonium group, which is evident from the O-C-C-N torsion angles that range from 47.8 to 67.8° (Table S6). A slight difference in torsion angle is also observed between the two symmetry independent molecules of Form 1, even though their conformations are the same, producing an RMSD value of only 0.041 Å. The Type A solvates all share the same conformation, with RMSD values less than 0.04 Å, and only a slight variation in O-C-C-N torsion angle of 5–7° (Table S6). The Type A solvates also have the same conformation as Form 3, with RMSD values around 0.2 Å. Given that these forms share similar structural motifs (Figure S5), this conformational similarity suggests that the Type A solvates may be modifications of Form 3, adapted to allow for the incorporation of solvent within the lattice. To evaluate the relative energy between *gauche*- and *anti*-conformation in mexiletine DFT-D calculations were performed starting from the experimentally observed conformations. The two minorly different conformations from Form 1 and one of the conformations in Form 2 all optimize to the same *gauche*-conformer, while Form 3 and solvent-free Type A solvate form optimize to a slightly different *gauche*-conformer (+2 kJ mol^{-1}). More interestingly, the *anti*-conformer of Form 2 was calculated to be significantly less stable (+39 kJ mol^{-1}) than the most stable *gauche* conformer, thus a significant energy input is required to form this conformation. This correlates well with the need for sublimation temperatures to generate Form 2.

Crystal Structure Prediction

Alongside experimental techniques, the polymorph landscape of mexiletine hydrochloride was also investigated by crystal structure prediction for structures with $Z' = 1$ in the 20 most common space groups. Structures were ranked initially using a force-field approach designed by AstraZeneca, AZ-FF.[13] The 1000 most stable structures were fully re-optimized and ranked in terms of their relative energies, using dispersion-corrected density functional theory. A detailed description of the calculation procedure can be found in the ESI. Of the 1000 structures in the final ranking, 77 were found to be within 10 kJ mol^{-1} of the minimum energy form, which corresponds to structures that may potentially be accessible using standard experimental techniques (10 kJ mol^{-1} was chosen to give some tolerance over previous estimates of 7 kJ mol^{-1} for accessible forms[45]). The relative energies of these forms at 0 K are shown in Figure 18, as a function of density. Predicted structures that are isostructural with known forms are highlighted in red. For comparison, the relative energies of the known Forms 1, 2, 3 and the Type A solvent-free form were calculated from their crystal structures and are also plotted in red. The solvent-free Type A form has a much lower density and so for clarity, its relative energy is shown in a separate plot. This calculation predicted structures with only one mexiletine molecule per asymmetric unit and did not consider solvated forms. As a result, neither Form 1 nor the Type B solvates are expected to appear in the CSP results, as they both have two molecules per asymmetric unit. Despite having one molecule per asymmetric unit, neither Form 2 nor the Type A solvates were predicted by the calculation, likely due to their disorder, and large voids, respectively. However, Form 2 is closely related to predicted Form 314. Form 3 was successfully predicted by the calculation and is isostructural with predicted Form 973.

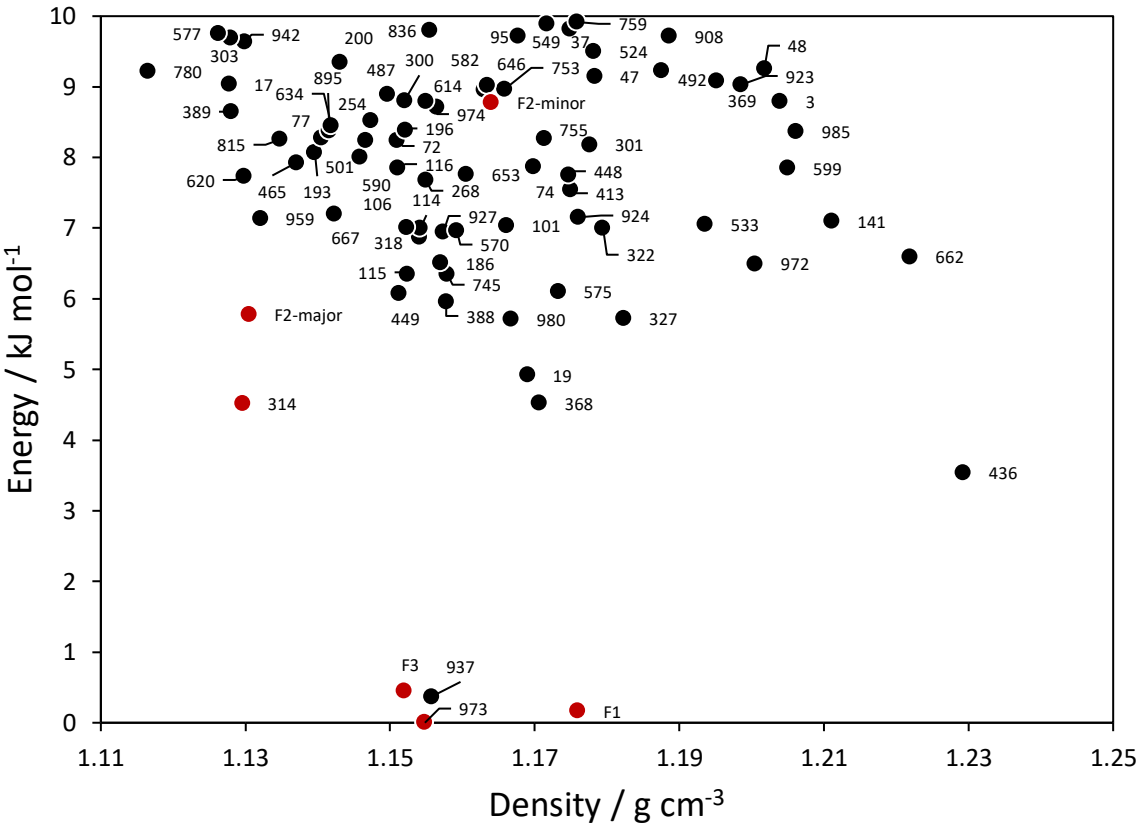
Energy / kJ mol-1
Density / g cm-3
10
9
8
7
6
5
4
3
2
1
0
1.11
1.13
1.15
1.17
1.19
1.21
1.23
1.25
577
942
303
200
836
95
549
37
759
908
48
780
17
634
895
487
300
582
646
753
524
47
492
923
369
3
389
77
254
614
974
F2-minor
815
196
72
755
301
985
501
116
653
448
599
620
465
193
590
106
114
268
74
413
959
667
318
927
101
924
533
141
570
322
662
972
115
186
745
575
F2-major
449
388
980
327
19
314
368
436
F3
937
973
F1

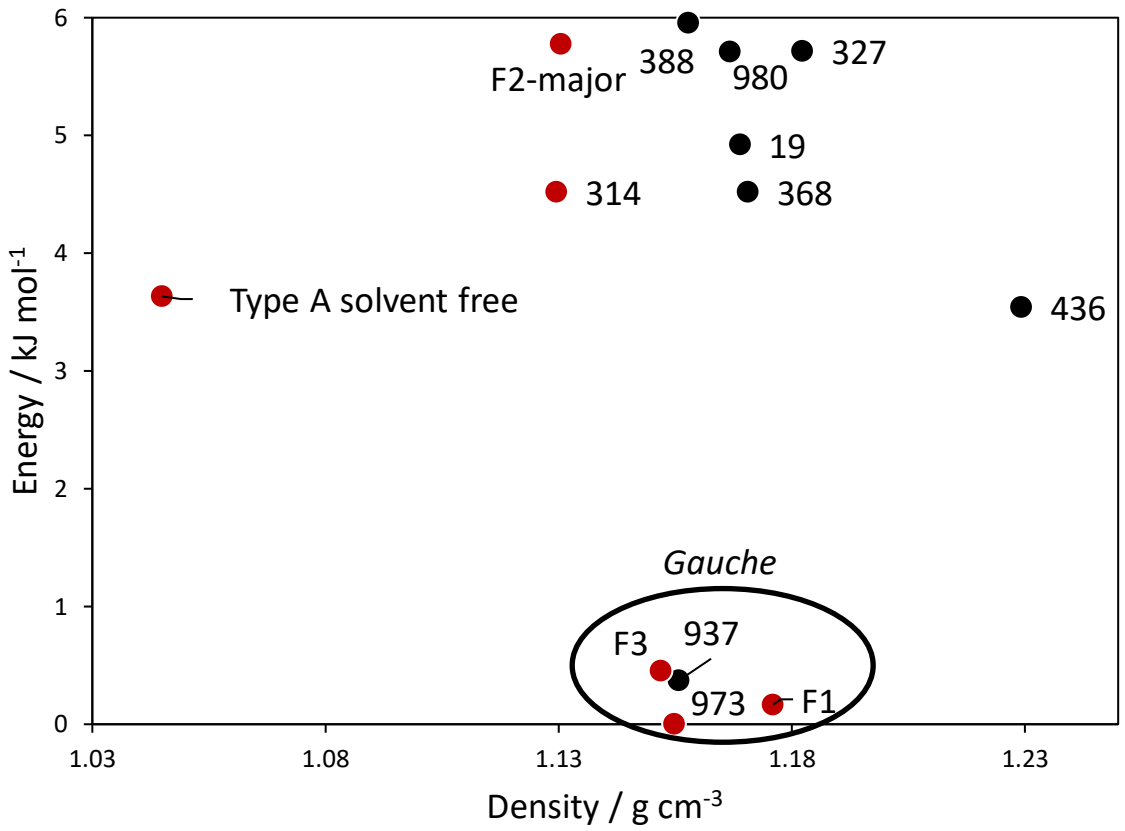

Figure 18. The relative energies of the predicted crystal structures of mexiletine hydrochloride, compared to the known forms. The experimental forms are labelled F1-F3 and the predicted structures are numbered. Experimental forms, and the predicted forms that are isostructural with known forms, are highlighted in red. Form 2 is closely related to calculated form 314 while Form 3 and calculated form 973 are isostructural.

The calculated energies of the known forms reflect the experimental DSC data. Form 1 has the lowest relative energy of the four experimental polymorphs, at 0.2 kJ mol^{-1} and Form 3 is close in energy to Form 1 at 0.4 kJ mol^{-1}. Likely due to the presence of large voids, the Type A solvent-free form is much higher in energy at 3.6 kJ mol^{-1} although, it is still lower energy than most of the predicted structures. Finally, as expected, the entropically stabilised Form 2 has the highest relative energy at 5.8 and 8.8 kJ mol^{-1} optimized from major and minor forms

of disordered structure, respectively. The very small energy difference between Forms 1 and 3 may explain why they often crystallise concomitantly and DSC data suggest that Form 3 may be more stable than Form 1, above the Form 1 to 2 transition temperature.

There is a very small difference in energy between Form 3 and its isostructural predicted Form 973, which derives from small differences in unit cell dimensions, and is within the accuracy of this technique. However, there is a larger difference in energy between the disordered Form 2 and the closely related predicted Form 314. The only structural difference between these two structures is that the molecules in Form 314 are spaced slightly wider apart in the b-direction, leading to a lower density. The Mercury packing similarity analysis of Forms 2 and 314 shows that all 20 molecules in the group overlap, with an RMSD of 0.1851 Å, indicating that the packing arrangements are essentially the same. Similarly, the molecular conformation in Form 314 is identical to that of the *anti*-periplanar molecule in Form 2, with an RMSD of only 0.0984 Å. The lower energy of Form 314 may therefore derive from the lack of disorder at 0 K.

Predicted Form 937 stands out because it is at very low energy, at 0.4 kJ mol^{-1}. This form was not observed experimentally but is in fact a high symmetry version of Form 3, in which the *a*-axis has been halved (Figure S13). The density of Form 937 is slightly higher than Form 3 but other than that, the packing arrangements of the two forms are very similar. The molecular conformation in Form 314 is also identical to Form 3, with an RMSD of only 0.0322 Å. It seems that the predicted Form 937 is an idealized version of Form 3, which is prohibited from crystallising experimentally either due to defects during the nucleation or growth steps, or symmetry breaking as a result of optimisation of intermolecular interactions and dynamical effects.

Although the Type A solvent-free form was not found in this CSP search, predicted Form 662 has the same space group and similar hydrogen bonding motifs. As in the Type A

structures, there are three hydrogen bonds per chloride ion that produce a hydrogen-bonded mexiletine polymer down the crystallographic *c*-axis, in which the molecules are arranged in a square formation (Figure S14). However, only 1 out of a group of 20 molecules overlapped when two structures were overlaid, with an RMSD value of 0.545 Å showing that their packing arrangements are very different. The main difference between Form 662 and the solvent-free Type A form is the density. Due to a lack of voids, Form 662 is significantly more dense, at 1.22 g cm^{-3}, compared to 1.045 g cm^{-3} for the solvent-free Type A form. Even the Type A methanol solvate, which does not have empty voids, is less dense than Form 662 at 1.15 g cm^{-3}.

In Form 662, the mexiletine molecule adopts an *anti*-periplanar conformation that is only observed in the highest energy experimental polymorph, Form 2. This *anti*-periplanar conformation is observed in all the predicted structures, apart from Form 924 (+7.2 kJ mol^{-1}), and the two forms that are isostructural with Form 3: Forms 973 and 937. Form 924 is markedly different to all the known forms in terms of both molecular conformation and packing arrangement. The *gauche* molecule in Form 2 has the most similar conformation to Form 924, although an RMSD value of 0.485 Å shows the two conformations are statistically different. Similarly, the Mercury packing similarity analysis showed that only 2 or 3 molecules of Form 924 overlap with Forms 1, 2 and 3, out of a group of 20. Although the hydrogen bonding motifs in Form 924 are very similar to Form 3, the change in molecular conformation causes the molecules to pack together very differently (Figure 19).

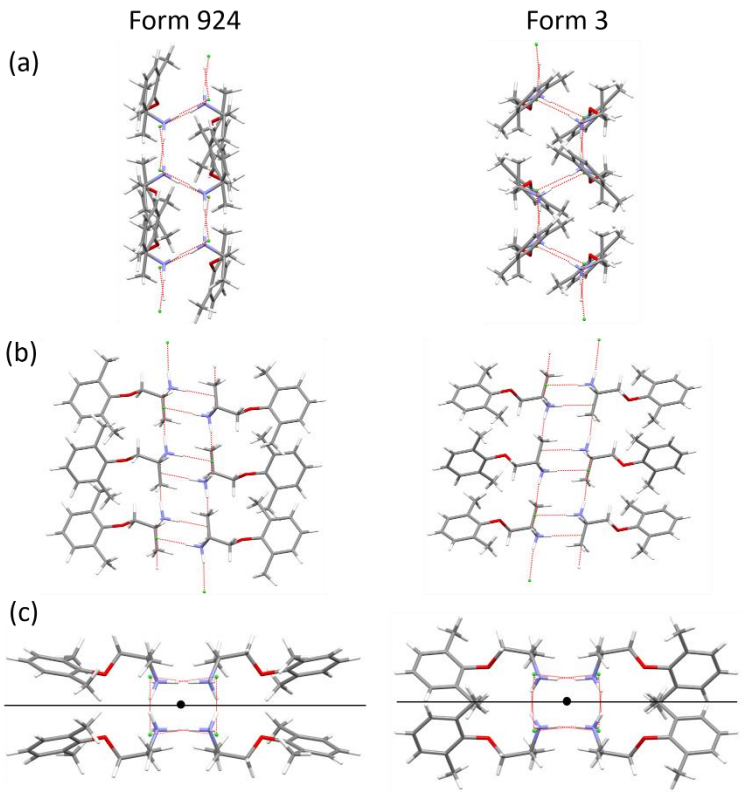

Figure 19. The packing arrangement in predicted Form 924 of mexiletine, compared to Form 3, viewed down the (a) *a*-axis, (b) *b*-axis and (c) *c*-axis. In image (c), the centres of inversion are shown as black circles and the *c*-glide planes are shown as black lines. There are more glide planes in Form 924, which have been omitted for clarity.

A *gauche* conformation is observed in both the lowest energy predicted Forms 973 and 937, as highlighted in Figure 18. All the other predicted structures are significantly higher in energy, and apart from one exception, have an *anti*-periplanar conformation. These results are in concordance with the predictions that the *anti*-periplanar conformation is higher energy than the *gauche* one, and mirror experimental observations in which an *anti*-periplanar conformation is only observed in the highest energy Form 2. This high energy, *anti*-periplanar conformation is thus probably difficult to nucleate under ambient conditions and therefore, it is unlikely that any of the predicted forms would be accessible using standard experimental techniques. The only possible exception is Form 436, which is very dense and has a low relative

energy of 3.5 kJ mol^{-1}. Although this form includes an *anti*-periplanar conformation, the barrier to nucleating the less stable conformation may be overcome by crystallising mexiletine hydrochloride under high pressure.[46] Taken as a whole, the CSP results correctly identify Form 3 as the most stable $Z' = 1$ polymorph under ambient conditions. The room temperature stable $Z' = 2$ Form 1 is denser and lower in energy, confirming it as the thermodynamic form at room temperature. The high temperature Form 2 in particular is entropically stabilised and appears high on the CSP landscape at 0 K. The absence of other undiscovered low energy polymorphs in the CSP solid-form landscape gives confidence that the experimental screening has identified all the accessible $Z' = 1$ non-solvated forms of mexiletine hydrochloride.

HIGH PRESSURE CRYSTALLISATION

The high density of relatively high stability of calculated Form 436 of mexiletine HCl suggests that it may be possible to isolate this additional form at high pressure in a similar way to the recent isolation of the predicted Form 3 of iproniazid.[47] To explore this hypothesis, a single crystal of Form 2 was compressed to 3.56 GPa in a diamond anvil cell. Form 2 was chosen for this experiment because it has the same *anti*-periplanar conformation as Form 436, which minimises the molecular rearrangement required to carry out the transformation. Although the crystal remained intact under high pressure, the crystal quality reduced dramatically, and it was no longer birefringent (Figure S15). A slight expansion of the unit cell was observed when the crystal was compressed (Table 8). Due to the reduced crystal quality and the shading effect of the DAC gasket, the diffraction at high pressure was very weak and the resolution was poor, which may have led to the discrepancy in unit cell dimensions. Similarly, the high-pressure data were recorded at room temperature whereas the ambient-pressure structure of Form 2 was recorded at 120 K, which may also have contributed to the expansion of the unit cell. Although predicted Form 436 was not observed in this experiment,

these changes in unit cell dimensions suggest that there is significant potential for further study of mexiletine HCl at high pressure.

Table 8. Unit cell dimensions obtained by compressing a crystal of Form 2 of mexiletine HCl to 3.56 GPa. Data were recorded at room temperature in a diamond anvil cell.

	Form 2 120K	**Form 2 compressed to 3.56 GPa**
a/Å	17.8741(14)	18.680(3)
b/Å	18.6782(15)	18.125(9)
c/Å	7.3462(7)	7.398(4)
α/°	90	90
β/°	90	90.04(10)
γ/°	90	90

Crystal Interaction (CrysIn) Analysis

A final piece of analysis was performed using CrysIn, evaluating intermolecular interactions based on DFT-D calculations on dimer structures extracted from the optimized crystal packing structures. Comparing the ionic interactions in the non-solvated forms of mexiletine hydrochloride it is found that the *anti*-conformation of Form 2 has the shortest and strongest NH···Cl ion-pairing (2.07-2.10 Å) among these. Thus, the relatively high conformational energy of the *anti*-conformation is to some extent compensated by a stronger ionic coordination. The *gauche*-conformation of Form 2 has three more unequal NH···Cl ion-pairing distances (2.07-2.30 Å), thus appears less efficient. Similarly, Form 3 has NH···Cl ion-pairing distances of 2.10-2.17 Å while in Type A solvent-free form the NH···Cl ion-pairing distances are 2.08-2.18 Å. Form 1 has the both shortest and longest NH···Cl ion-pairing interactions (2.00-2.31 Å, and 2.04-2.35 Å for the two different conformations, respectively), but in total this creates the weakest ionic network. These differences in NH···Cl ion-pairing may be what

is observed in the IR-spectra where Form 1 appears to have most diversity in peak positions (*vide supra*).

CONCLUSIONS

In conclusion, this approach to the solid forms landscape of mexiletine hydrochloride has consolidated previous studies and revealed that mexiletine hydrochloride exhibits at least three non-solvated polymorphs, termed Forms 1, 2 and 3, and two families of isomorphic channel solvates, termed Types A and B. In both solvate families, the drug framework acts as a host and remains mostly unchanged with the inclusion of different guests. The solvates differ in their value of Z', with Type A having one molecule per asymmetric unit and Type B having two. The two families are related by similar packing arrangements and hydrogen bonding motifs, but the Type B structure is significantly more complex. We have found eleven modifications of each solvate, including a wide range of different solvents with aliphatic, aromatic, polar and non-polar functionalities. Mexiletine hydrochloride was previously known to be an enantiotropic system, in which Form 1 is stable at low temperatures and Form 2 is stable at high temperatures. Interestingly, all three polymorphs are related enantiotropically and Form 3 is the thermodynamically stable polymorph between 148 °C (transition of Form 1 to 2) and 167 °C (transition of Form 3 to 2). This study reports for the first time, the single-crystal structure of Form 2, which was accessed by sublimation and is structurally related to the Type B solvates. The structure of each polymorph was characterised by PXRD and IR spectroscopy, and the composition of the solvates was investigated using ^{13}C solid-state NMR spectroscopy, as the solvent was often too disordered to diffract X-rays. The experimental results were supported using computational tools including Mercury and PolySNAP, which compared the structures and quantified their similarity. Finally, a crystal structure prediction study replicated many of the structural and hydrogen bonding motifs seen in the experimental

forms, including the prediction of Forms 2 and 3. This calculation showed that Forms 1 and 3 are close together in energy whilst Form 2 is significantly less stable at 0 K. This result mirrors experimental trends in which Form 3 crystallised concomitantly with Form 1, and Form 2 was only accessible at high temperatures. Most of the predicted forms include an *anti*-periplanar conformation of mexiletine's aromatic chain, which was only observed experimentally in the high temperature stable Form 2. The inclusion of this high energy conformation likely explains why very few of the predicted forms crystallised experimentally.

Mexiletine hydrochloride is an example showing the importance of a thorough solid-state study in the pharmaceutical sciences. With the tight restrictions on residual solvent given by the ICH guideline Q3A, the observed new solvent families pose a risk of carrying potentially toxic solvent through the manufacturing process into drug administration. This study clearly shows that only the meticulous application of various solid-state and computational techniques can give the full picture of solvent inclusion and de-risk the manufacture of novel pharmaceuticals.

ASSOCIATED CONTENT

Supporting Information

The ESI contains further information on the materials and instrumentation used in this study, plus full experimental details of the crystallisation and characterisation of solid forms, computational analyses, and crystal structure prediction. Supplementary figures include PXRD patterns, IR spectra, solid-state ^{13}C NMR spectra, predicted and experimental crystal structures, O-C-C-N torsion angles in all experimental crystal structures compared to the CSD, and full crystallographic information for all the novel solid forms of mexiletine hydrochloride identified in this work.

Accession Codes

CCDC 2100536-2100544 contain the supplementary crystallographic data for this paper. The data can be obtained free of charge from The Cambridge Crystallographic Data Centre via www.ccdc.cam.ac.uk/structures.

AUTHOR INFORMATION

Corresponding Author

* Jonathan W. Steed, email: jon.steed@durham.ac.uk

Present Addresses

† The present address of these authors differs from where the research was conducted. Present addresses are given below.

David J. Berry: Medicines Manufacturing Innovation Centre, Centre for Process Innovation, Wilton Centre, Wilton, Redcar, TS10 4RF.

ORCID

Jessica L. Andrews: 0000-0003-1894-2437

Sten O. Nilsson Lill: 0000-0003-4818-8084

Stefanie Freitag-Pohl: 0000-0002-1423-8103

David C. Apperley: 0000-0001-7102-0314

Dmitry S. Yufit: 0000-0002-7208-1212

Andrei S. Batsanov: 0000-0002-4912-0981

Matthew T. Mulvee 0000-0002-5108-3227

Katharina Edkins: 0000-0002-6885-5457

David J. Berry: 0000-0001-6321-7379

James F. McCabe 0000-0002-6062-2253

Michael R. Probert: 0000-0002-2412-7917

Jonathan W. Steed: 0000-0002-7466-7794

Author Contributions

The manuscript was written through contributions of all authors. All authors have given approval to the final version of the manuscript.

Notes

The authors declare no competing financial interest.

ACKNOWLEDGMENT

We would like to thank Mr. W. Douglas Carswell for his assistance with DSC measurements, Dr. Charlie McMonagle, Newcastle University, for assistance with the high-pressure experiments and the Engineering and Physical Sciences Research Council for funding, through the SOFI CDT and Durham University. We also thank and the Diamond Light Source

(Oxfordshire, UK) for an award of instrument time on the Station I19 (MT 11145) and the instrument scientists for support.

REFERENCES

1. Brittain, H. G., *Polymorphism in Pharmaceutical Solids*. 2nd ed.; CRC Press: 2016.
2. Bernstein, J., In *Polymorphism in Molecular Crystals*, Clarendon Press: Oxford, 2002; pp 240-256.
3. Bauer, J.; Spanton, S.; Henry, R.; Quick, J.; Dziki, W.; Porter, W.; Morris, J., Ritonavir: an extraordinary example of conformational polymorphism. *Pharm. Res.* **2001**, *18*, 859-866.
4. Saurabh, G.; Kaushal, C., Pharmaceutical solid polymorphism in abbreviated new drug application (ANDA)-a regulatory perspective. *J. Chem. Pharm. Res* **2011**, *3*, 6-17.
5. Bernstein, J., In *Polymorphism in Molecular Crystals*, Oxford University Press: 2002; pp 297-307.
6. Florence, A. J., Polymorph screening in pharmaceutical development. *Eur. Pharm. Rev.* **2010**, *4*, 28-33.
7. Lee, E. H., A practical guide to pharmaceutical polymorph screening & selection. *Asian J. Pharm. Sci.* **2014**, *9*, 163-175.
8. Morissette, S. L.; Almarsson, Ö.; Peterson, M. L.; Remenar, J. F.; Read, M. J.; Lemmo, A. V.; Ellis, S.; Cima, M. J.; Gardner, C. R., High-throughput crystallization: polymorphs, salts, co-crystals and solvates of pharmaceutical solids. *Adv. Drug Deliv. Rev.* **2004**, *56*, 275-300.
9. Tyler, A. R.; Ragbirsingh, R.; McMonagle, C. J.; Waddell, P. G.; Heaps, S. E.; Steed, J. W.; Thaw, P.; Hall, M. J.; Probert, M. R., Encapsulated Nanodroplet Crystallization of Organic-Soluble Small Molecules. *Chem* **2020**, *6*, 1755-1765.
10. Price, S. L., The computational prediction of pharmaceutical crystal structures and polymorphism. *Adv. Drug Deliv. Rev.* **2004**, *56*, 301-319.
11. Adjiman, C. S.; Brandenburg, J. G.; Braun, D. E.; Cole, J.; Collins, C.; Cooper, A. I.; Cruz-Cabeza, A. J.; Day, G. M.; Dudek, M.; Hare, A.; Iuzzolino, L.; McKay, D.; Mitchell, J. B. O.; Mohamed, S.; Neelamraju, S.; Neumann, M.; Nilsson Lill, S.; Nyman, J.; Oganov, A. R.; Price, S. L.; Pulido, A.; Reutzel-Edens, S.; Rietveld, I.; Ruggiero, M. T.; Schön, J. C.; Tsuzuki, S.; van den Ende, J.; Woollam, G.; Zhu, Q., Applications of crystal structure prediction – organic molecular structures: general discussion. *Faraday Discussions* **2018**, *211*, 493-539.
12. Mortazavi, M.; Hoja, J.; Aerts, L.; Quéré, L.; van de Streek, J.; Neumann, M. A.; Tkatchenko, A., Computational polymorph screening reveals late-appearing and poorly-soluble form of rotigotine. *Communications Chemistry* **2019**, *2*, 70.
13. Broo, A.; Nilsson Lill, S. O., Transferable force field for crystal structure predictions, investigation of performance and exploration of different rescoring strategies using DFT-D methods. *Acta Crystallographica Section B* **2016**, *72*, 460-476.
14. Abounassif, M. A.; Mian, M. S.; Aziz Mian, N. A., Analytical Profile of Mexiletine Hydrochloride. In *Analytical Profiles of Drug Substances*, Florey, K., Ed. Academic Press: 1991; Vol. 20, pp 433-474.
15. Mehvar, R.; Brocks, D. R.; Vakily, M., Impact of stereoselectivity on the pharmacokinetics and pharmacodynamics of antiarrhythmic drugs. *Clin. Pharmacokinet.* **2002**, *41*, 533-558.

16. Bredikhina, Z. A.; Kurenkov, A. V.; Krivolapov, D. B.; Bredikhin, A. A., Stereoselective crystallization of 3-(2,6-dimethylphenoxy)propane-1,2-diol: preparation of the single-enantiomer drug mexiletine. *Tetrahedron Asymm.* **2015**, *26*, 577-583.
17. Turgeon, J.; Uprichard, A. C. G.; Belanger, P. M.; Harron, D. W. G.; Grechbelanger, O., Resolution and electrophysiological effects of mexiletine enantiomers. *J. Pharm. Pharmacol.* **1991**, *43*, 630-635.
18. Franchini, C.; Cellucci, C.; Corbo, F.; Lentini, G.; Scilimati, A.; Tortorella, V.; Stasi, F., Stereospecific synthesis and absolute-configuration of mexiletine. *Chirality* **1994**, *6*, 590-595.
19. Aav, R.; Parve, O.; Pehk, T.; Claesson, A.; Martin, I., Preparation of highly enantiopure stereoisomers of 1-(2,6-dimethylphenoxy)-2-aminopropane (mexiletine). *Tetrahedron-Asymmetry* **1999**, *10*, 3033-3038.
20. Koszelewski, D.; Pressnitz, D.; Clay, D.; Kroutil, W., Deracemization of Mexiletine Biocatalyzed by ω-Transaminases. *Org. Lett.* **2009**, *11*, 4810-4812.
21. Koszelewski, D.; Muller, N.; Schrittwieser, J. H.; Faber, K.; Kroutil, W., Immobilization of omega-transaminases by encapsulation in a sol-gel/celite matrix. *J. Mol. Catal. B-Enzym.* **2010**, *63*, 39-44.
22. Carocci, A.; Franchini, C.; Lentini, G.; Loiodice, F.; Tortorella, V., Facile entry to (-)-(R)- and (+)-(S)-mexiletine. *Chirality* **2000**, *12*, 103-106.
23. Carbonara, G.; Carocci, A.; Fracchiolla, G.; Franchini, C.; Lentini, G.; Loiodice, F.; Tortorella, P., H-1-NMR determination of the enantiomeric excess of the antiarrhythmic drug Mexiletine by using mandelic acid analogues as chiral solvating agents. *Arkivoc* **2004**, *5*, 5-25.
24. Aboulenein, H. Y.; Rothchild, R.; Sinnema, A., Nmr-studies of drugs - chiral solvating agents for direct determination of enantiomeric excess of the cardiac antiarrhythmic, mexiletine. *Spectr. Lett.* **1992**, *25*, 1367-1385.
25. Namespetra, A. M.; Hirsh, D. A.; Hildebrand, M. P.; Sandre, A. R.; Hamaed, H.; Rawson, J. M.; Schurko, R. W., 35Cl solid-state NMR spectroscopy of HCl pharmaceuticals and their polymorphs in bulk and dosage forms. *CrystEngComm* **2016**, *18*, 6213-6232.
26. Hildebrand, M.; Hamaed, H.; Namespetra, A. M.; Donohue, J. M.; Fu, R.; Hung, I.; Gan, Z.; Schurko, R. W., ^{35}Cl solid-state NMR of HCl salts of active pharmaceutical ingredients: structural prediction, spectral fingerprinting and polymorph recognition. *CrystEngComm* **2014**, *16*, 7334-7356.
27. Sivy, J.; Kettmann, V.; Fresova, E., Structure of 1-(2,6-dimethylphenoxy)-2-propanamine hydrochloride. *Acta Crystallogr., Sect. C: Cryst. Struct. Commun.* **1991**, *47*, 2695-2696.
28. Kiss, A.; Repasi, J., Investigation of polymorphism of mexiletine hydrochloride by Fourier transform infrared and differential scanning calorimetric techniques. *Analyst* **1993**, *118*, 661-664.
29. Kuhnert, M.; Seidel, D.; Unterkircher, G., Mexiletine hydrochloride, oxypendyl dihydrochloride, penbutolol sul fate and pirprofen. *Sci. Pharm.* **1987**, *55*, 13-25.
30. Desiraju, G. R., Polymorphism: The Same and Not Quite the Same. *Cryst. Growth Des.* **2008**, *8*, 3-5.
31. Bernstein, J., Polymorphism - A Perspective. *Cryst. Growth Des.* **2011**, *11*, 632-650.
32. Stephenson, G. A.; Groleau, E. G.; Kleemann, R. L.; Xu, W.; Rigsbee, D. R., Formation of Isomorphic Desolvates: Creating a Molecular Vacuum. *J. Pharm. Sci.* **1998**, *87*, 536-542.
33. Bērziņš, A.; Trimdale, A.; Kons, A.; Zvaniņa, D., On the Formation and Desolvation Mechanism of Organic Molecule Solvates: A Structural Study of Methyl Cholate Solvates. *Cryst. Growth Des.* **2017**, *17*, 5712-5724.

34. Yu, L., Survival of the fittest polymorph: how fast nucleater can lose to fast grower. *CrystEngComm* **2007**, *9*, 847-851.
35. Barr, G.; Dong, W.; Gilmore, C. J., PolySNAP3: a computer program for analysing and visualizing high-throughput data from diffraction and spectroscopic sources. *J. Appl. Crystallogr.* **2009**, *42*, 965-974.
36. Barr, G.; Dong, W.; Gilmore, C. J., PolySNAP: a computer program for analysing high-throughput powder diffraction data. *J. Appl. Crystallogr.* **2004**, *37*, 658-664.
37. Macrae, C. F.; Bruno, I. J.; Chisholm, J. A.; Edgington, P. R.; McCabe, P.; Pidcock, E.; Rodriguez-Monge, L.; Taylor, R.; van de Streek, J.; Wood, P. A., Mercury CSD 2.0 - new features for the visualization and investigation of crystal structures. *J. Appl. Crystallogr.* **2008**, *41*, 466-470.
38. Chisholm, J. A.; Motherwell, S., COMPACK: a program for identifying crystal structure similarity using distances. *J. Appl. Crystallogr.* **2005**, *38*, 228-231.
39. Steed, J. W.; Atwood, J. L., In *Supramol. Chem.*, 2nd ed.; John Wiley and Sons: 2009; pp 385-440.
40. Barbour, L. J., Crystal porosity and the burden of proof. *Chem. Commun.* **2006**, *11*, 1163-1168.
41. Turner, M. J.; McKinnon, J. J.; Jayatilaka, D.; Spackman, M. A., Visualisation and characterisation of voids in crystalline materials. *CrystEngComm* **2011**, *13*, 1804-1813.
42. Spek, A. L., PLATON SQUEEZE: a tool for the calculation of the disordered solvent contribution to the calculated structure factors. *Acta Crystallogr. Sect. C-Struct. Chem.* **2015**, *71*, 9-18.
43. Borowski, P.; Gac, W.; Pulay, P.; Woliński, K., The vibrational spectrum of 1,4-dioxane in aqueous solution – theory and experiment. *New J. Chem.* **2016**, *40*, 7663-7670.
44. Cruz-Cabeza, A. J.; Bernstein, J., Conformational Polymorphism. *Chem. Rev.* **2014**, *114*, 2170-2191.
45. Nyman, J.; Day, G. M., Static and lattice vibrational energy differences between polymorphs. *CrystEngComm* **2015**, *17*, 5154-5165.
46. Neumann, M. A.; van de Streek, J.; Fabbiani, F. P. A.; Hidber, P.; Grassmann, O., Combined crystal structure prediction and high-pressure crystallization in rational pharmaceutical polymorph screening. *Nature Commun.* **2015**, *6*, 7793.
47. Taylor, C. R.; Mulvee, M. T.; Perenyi, D. S.; Probert, M. R.; Day, G. M.; Steed, J. W., Minimizing Polymorphic Risk through Cooperative Computational and Experimental Exploration. *J. Am. Chem. Soc.* **2020**, *142*, 16668-16680.

For Table of Contents Use Only:

De-risking the Polymorph Landscape: The Complex Polymorphism of Mexiletine Hydrochloride

Jessica L. Andrews, Sten O. Nilsson Lill, Stefanie Freitag-Pohl, David C. Apperley, Dmitry S. Yufit, Andrei S. Batsanov, Matthew T. Mulvee, Katharina Edkins, James F. McCabe, David J. Berry, Michael R. Probert and Jonathan W. Steed.

TOC GRAPHIC

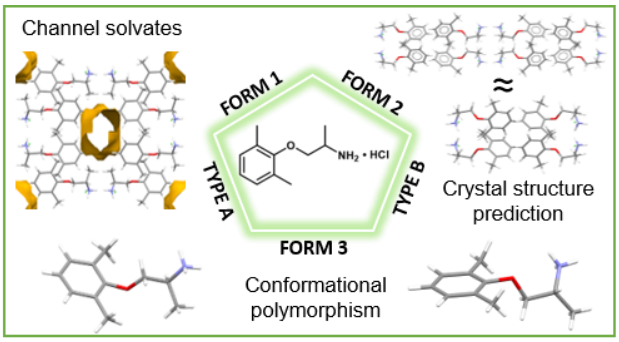

SYNOPSIS

The complex solid form landscape of mexiletine hydrochloride has been carefully mapped revealing five types of solid form: three mutually enantiotropically related anhydrous polymorphs, and two families of isomorphous channel solvates. Experimental screening and computational crystal structure prediction go hand-in-hand to demonstrate a link between molecular conformation and polymorph stability.